REPORT DOCUMENTATION PAGE

1. REPORT DATE *(DD-MM-YYYY)* 09-05-2011	**2. REPORT TYPE** Conference Paper	**3. DATES COVERED** *(From - To)*

4. TITLE AND SUBTITLE

Investigation of Density Perturbations in Molecular Nitrogen Formed by Pulsed Optical Lattices

5a. CONTRACT NUMBER

5b. GRANT NUMBER

5c. PROGRAM ELEMENT NUMBER

6. AUTHOR(S)

Barry Cornella, Trey Quiller, Sergey Gimelshein, Taylor Lilly and Andrew Ketsdever

5d. PROJECT NUMBER

5f. WORK UNIT NUMBER
50260532

7. PERFORMING ORGANIZATION NAME(S) AND ADDRESS(ES)

Air Force Research Laboratory (AFMC)
AFRL/RZSA
10 E. Saturn Blvd.
Edwards AFB CA 93524-7680

8. PERFORMING ORGANIZATION REPORT NUMBER

AFRL-RZ-ED-TP-2011-160

9. SPONSORING / MONITORING AGENCY NAME(S) AND ADDRESS(ES)

Air Force Research Laboratory (AFMC)
AFRL/RZS
5 Pollux Drive
Edwards AFB CA 93524-7048

10. SPONSOR/MONITOR'S ACRONYM(S)

11. SPONSOR/MONITOR'S NUMBER(S)
AFRL-RZ-ED-TP-2011-160

12. DISTRIBUTION / AVAILABILITY STATEMENT

Approved for public release; distribution unlimited (PA #11194).

13. SUPPLEMENTARY NOTES
For presentation at the 42nd AIAA Thermophysics Conference, Honolulu, HI 27-30 June 2011.

14. ABSTRACT

A complimentary experimental/numerical investigation on the effect of counter-propagating pulsed lasers on molecular nitrogen was conducted. The experiment verified published theoretical predictions of the effect of laser intensity and gas pressure on the magnitude of induced density perturbations in the gas using a coherent Rayleigh-Brillouin scattering technique. The investigation further verified the use of a modified version of the SMILE DSMC code for more robust prediction of the effect of a non-resonant pulsed optical lattice on a neutral gas. The ambient pressure of molecular nitrogen was varied from 100 torr to 760 torr, and the pump laser energy was varied from 2 mJ to 25 mJ per pulse. The resulting scattered signal from the experiment was measured and compared with numerical predictions. Assuming that the signal of the experiment is proportional to the probe intensity and the square of the density perturbations induced by the pump lasers, the results of the experiment qualitatively support both theoretical predictions and numerical simulations.

15. SUBJECT TERMS

16. SECURITY CLASSIFICATION OF:			**17. LIMITATION OF ABSTRACT**	**18. NUMBER OF PAGES**	**19a. NAME OF RESPONSIBLE PERSON** Dr. Andrew D. Ketsdever
a. REPORT Unclassified	**b. ABSTRACT** Unclassified	**c. THIS PAGE** Unclassified	SAR	9	**19b. TELEPHONE NUMBER** *(include area code)* N/A

Investigation of Density Perturbations in Molecular Nitrogen Formed by Pulsed Optical Lattices

Barry Cornella [*], Trey Quiller[†], Sergey Gimelshein[‡],
ERC Inc., Edwards AFB, CA 93524, USA,

Taylor Lilly[§], and Andrew Ketsdever[**]
Air Force Research Laboratory, Edwards AFB, CA 93524, USA

A complimentary experimental/numerical investigation on the effect of counter-propagating pulsed lasers on molecular nitrogen was conducted. The experiment verified published theoretical predictions of the effect of laser intensity and gas pressure on the magnitude of induced density perturbations in the gas using a coherent Rayleigh-Brillouin scattering technique. The investigation further verified the use of a modified version of the SMILE DSMC code for more robust prediction of the effect of a non-resonant pulsed optical lattice on a neutral gas. The ambient pressure of molecular nitrogen was varied from 100 torr to 760 torr and the pump laser energy was varied from 2 mJ to 25 mJ per pulse. The resulting scattered signal from the experiment was measured and compared with numerical predictions. Assuming that the signal of the experiment is proportional to the probe intensity and the square of the density perturbations induced by the pump lasers, the results of the experiment qualitatively support both theoretical predictions and numerical simulations.

Nomenclature

c	=	speed of light = 299,792,458 [m/s]	t	=	time [s]
D	=	laser diameter (FWHM) [m]	U	=	potential energy [J]
E	=	electric field strength [V/m]	α	=	static polarizability [C m^2 V^{-1}]
F	=	force [N]	ε_0	=	electric constant = 8.854187817... x10^{-12}
$FWHM$	=	full width half maximum			[A s V^{-1} m^{-1}]
I	=	laser intensity [W/m^2]	ξ	=	optical lattice velocity = Ω/q [m/s]
k	=	laser wave number [rad/m]	τ	=	laser pulse width (FWHM) [s]
m	=	particle mass [kg]	ω	=	laser frequency [rad/s]
q	=	lattice wave number = k_1-k_2 [rad/m]	Ω	=	lattice angular frequency = ω_1- ω_2 [rad/s]
r	=	radial position [m]			

I. Introduction

Pulsed optical lattice laser-gas interactions offer a potentially powerful tool for laser based neutral gas heating, acceleration, and modification. Most of the technique's advantages are due to the non-resonant nature of the laser-gas interaction, which could uniquely combine the general applicability of the approach to any test gas with the controllable nature of light interactions. This technique would yield a wide range of attainable temperatures and flow conditions. As compared with arc or laser powered discharge heating [1,2], non-resonant pulsed optical lattices offer the possibility to study high temperature gases without the ionization and molecular dissociation reactions associated with discharges. Traditional shock tubes, often used for high temperature flow studies [3,4], are characterized by very short interaction/probe times and significant deviations from thermal equilibrium. Deviations

---

from thermal equilibrium make the obtained results difficult to extrapolate to situations where the gas is close to equilibrium. One of the most robust approaches to producing heated gases is infrared laser powered homogeneous pyrolysis (IR LPHP). [5,6] In this method, energy is absorbed in a vibrational mode of the photosensitizer before being rapidly converted into translational modes through efficient relaxation processes.

A non-resonant optical lattice heating technique is expected to be superior to all of these techniques since it can theoretically provide a wider range of temperatures (in excess of 2000 K), be applicable to practically any gas species (non-resonant interaction), transfer energy from the laser directly into translational modes of the gas without intermediate steps, and maintain the main benefits of other techniques such as IR LPHP. These benefits include gas phase operation (homogeneity), the possibility to achieve spatial uniformity, and small operational volume. However, the realization of a non-resonant pulsed optical lattice heating technique relies on the seamless integration of theory and numerical prediction related to a multitude of disparate fields such as laser physics, optics, molecular gas dynamics, and traditional continuum fluid mechanics. This investigation looks at the use of one experiment, coherent Rayleigh-Brillouin scattering (CRBS), to validate analytical predictions and a numerical simulation method based on a modified version of the gas kinetic numerical simulation code SMILE. SMILE has been used to predict the modification of a neutral gas by several laser configurations [7-9] and is now compared directly with an experiment. The experiment and associated numerical method are initial steps on the path to laser based neutral gas heating, acceleration, and modification.

II.   Theoretical Framework and Numerical Method

The induced dipole gradient force on a particle originates from a potential associated with its immersion in a non-uniform electric field [10]. Since the magnitude of this force is traditionally small, it has so far only found a niche in the field of low temperature atomic research. The force is routinely utilized for confinement [11] and transposition [12,13] of neutral atoms in tailored light fields. In these applications, one or more lasers are used to create a spatially varying optical potential field. If two counter-propagating beams are arranged in a manner to create an optical standing wave, the axially periodic potential formed is referred to as a one dimensional optical lattice [14]. The majority of experiments utilizing the optical dipole force use a combination of continuous wave lasers and alkali metals or meta-stable noble gases. This combination allows for the tuning of the laser near well defined and isolated electronic resonances, which in turn increases the magnitude of the force in response to a given laser intensity. Using lasers further from resonance, the dipole force gains broader particle applicability [15], at the expense of the magnitude of the force. In order to regain some effectiveness, pulsed lasers can be used in lieu of continuous wave lasers to increase the instantaneous optical intensity. Higher optical intensity translates to a larger force along the potential gradient which in turn can strongly affect the particles in a gas. Applying a relatively high intensity, pulsed optical lattice to a continuum gas offers the use of the dipole force as a mechanism for creating a periodic density perturbation in the gas with a periodicity on the order of the laser wavelength [16,17]. This perturbation can then be used to probe various gas dynamic properties.

Detailed theory for the effect of an optical lattice on a collisional gas and the scattering of a probe beam off of the density perturbation formed by that interaction can be found in [16-19]. Background material can be found in closely related publications such as laser induced grating spectroscopy (LIGS) [20,21] and laser trapping and cooling [14,15,22].

The force acting on a polarizable medium in a non-uniform electric field is given by Boyd [10] as

$$F = -\nabla U = \left(-\alpha/2\right)\nabla E^2 \tag{1}$$

For anti-parallel, coherent, collimated laser pulses, the square of the electric field amplitude in the overlapping region is calculated as the superposition of two plane waves.

$$\begin{aligned} E^2\left(x,t\right) = {}& E_1^2 cos^2(k_1 x - \omega_1 t) + E_2^2 cos^2(k_2 x - \omega_2 t) + \\ & E_1 E_2\left[cos\left(\left(k_1 - k_2\right)x - \left(\omega_1 - \omega_2\right)t\right) + cos\left(\left(k_1 + k_2\right)x - \left(\omega_1 + \omega_2\right)t\right)\right] \end{aligned} \tag{2}$$

When $k_1 \approx -k_2$ and $\omega_1 \approx \omega_2$, the interference term of the field has two components: one with a relatively long spatial and short temporal period and the other with a short spatial and long temporal period. When the gradient of eqn. (2) is taken (per eqn. (1)), the portion with the long spatial period has a negligible impact. In addition, the fast oscillating terms (cos^2) can be time averaged to a constant value of 1/2. The resulting force acting on a particle within the potential region is given by

$$F = -\nabla U = \left(\alpha/2\right)\nabla\left[E_1 E_2\left(1 + cos\left(qx - \Omega t\right)\right)\right] \tag{3}$$

American Institute of Aeronautics and Astronautics

Note that Ω and q define the velocity of the optical potential wave, or lattice velocity, $\xi = \Omega/q$. The sign of Ω defines the direction of ξ. For this investigation the frequency of the two pulses was the same and therefore the lattice velocity was zero.

The intensity of the two laser pulses is assumed to have a Gaussian shape in both space and time which is described by

$$I(r,t) = I_{\max} \exp\left(-4\ln(2)\left[(t-t_o)^2\big/\tau^2 + r^2\big/D^2\right]\right) \Rightarrow E_0^2 = 2I\big/c\epsilon_0 \tag{4}$$

By substituting the laser intensity for the electric field magnitude, eqn. (3) in the axial direction becomes

$$F_x(x,r,t) = \alpha q\big/c\epsilon_0 \sqrt{I_1(r,t)I_2(r,t)} \; \sin(qx - \Omega t) \tag{5}$$

It should be noted that a gradient in the axial intensity profile caused by the temporal Gaussian shape can be neglected as $(2\pi/q)/(c\,\tau_{\text{fwhm}}) \ll 1$. This equation gives the force on an individual particle based on its location in space and the time relative to the center of the laser pulse's temporal envelope.

With the force on the particles within the gas evaluated, it can be inferred that the periodic nature of the force will induce a local area of higher density at the anti-nodes of the interference pattern. This perturbation in turn causes a periodic structure in the index of refraction of the gas, which is related to its density, effectively creating a grating which will scatter light. Given a certain set of parameters, such as the angle of the crossing pumps and the wavelength of the lasers, the scattered light will evolve as a coherent scatter off the grating, increasing the signal significantly over spontaneous processes [16,17]. It has been shown that the intensity of the returned light in a coherent Rayleigh scattering experiment is proportional to the intensity of the probing light and the square of the density perturbations in the gas [23]

$$I_{\text{sig}} \propto I_{\text{probe}} \delta\rho^2 \tag{6}$$

It has also been shown that the magnitude of the density perturbation should be proportional to the product of the pump laser intensities [23]

$$\delta\rho^2 \propto I_{\text{pump1}} I_{\text{pump2}} \tag{7}$$

Assuming the validity of eqn. (6), the numerical simulation package SMILE was used to calculate the density perturbation created by the periodic force given by eqn. (5). Since the force acting on the molecules directly affects the velocity distribution of the flow, a kinetic approach must be used to model the impact of the laser-molecule interaction on molecular trajectories. The kinetic code chosen was the Direct Simulation Monte Carlo (DSMC) code SMILE. The code was modified to include the non-resonant laser interaction described by eqn. (5). This modification used a Newtonian integration scheme to approximate the force on a molecule as a temporally and spatially varying acceleration which was considered constant over the duration of a simulation time step. Time steps were therefore reduced such that the species did not traverse appreciable fractions of the laser field or temporal pulse width in one time step. The SMILE code has been broadly applied and experimentally validated, see [24] and the references therein. Some of the features which have contributed to its broad applicability and validation (thus its choice for this study) were as follows: The VHS model [25] and majorant frequency scheme [26] are employed for modeling molecular collisions. The latter feature was particularly important for maintaining fidelity while reducing the time step to satisfy the laser interaction conditions. The Larsen-Borgnakke model [27] with temperature-dependent rotational and vibrational relaxation numbers is utilized for rotation/vibration-translation energy transfer.

Nitrogen was used as a test gas in this investigation. The polarizability to mass ratio of molecular nitrogen is 4.145 [10^{-15} C m^2 kg^{-1} V^{-1}]. The nominal set of conditions from which pressure and intensity were varied simulated a pair of 532 nm wavelength, 20 mJ per pulse, 15 μm FWHM pulse diameter, 5 ns FWHM pulse width lasers (maximum intensity of 1.47×10^{16} W/m^2) interacting with molecular nitrogen initially at a temperature 300 K and a number density of 24.475×10^{24} m^{-3}. The simulation domain was modeled axisymmetrically around the optical axis of the two anti-parallel, counter propagating laser pulses. These laser parameters are expected to be in a regime below optical breakdown threshold [28]. The pulses were assumed to have identical frequencies creating a lattice with zero velocity. In order to cover the temporal shape of the pulses, each pulse simulation ran from -τ to +τ where τ was assumed to be 5 ns (FWHM). Therefore, the total time for each simulation was 10 ns. With a laser pulse spatial length of approximately 1.5 m, the axial domain boundaries were considered periodic. The radial domain boundary was considered specular and assumed to represent a sufficiently small cross-section at the center of the laser focus that the surrounding volume was equally affected. The domain was nominally 1064 nm tall and ±332.5 nm wide. A diagram of the domain with an overlay of the maximum potential well depth ($T_{\text{plot}} = -2U/k$) is shown in Figure 1.

American Institute of Aeronautics and Astronautics

The first step in the simulation procedure was to populate the domain in the baseline ambient configuration with the appropriate gas properties. During the last 0.02% of the simulation, cells were sampled to give flow field values. With approximately 1,350 simulated particles per sample cell and 10 time steps averaged, the average statistical error is estimated at approximately 2%. For this analysis, there were four numerical parameter studies conducted. The first set of simulations used a constant maximum single pulse intensity of 3.685×10^{15} W/m^2 and varying gas pressure from 100 torr to 760 torr. The second used a maximum single pulse intensity of 2.211×10^{16} W/m^2 and similarly varying gas pressures. The third and fourth simulations used a constant gas pressure of 100 torr and 760 torr, respectively, and varying maximum single pulse intensities from 3.685×10^{15} W/m^2 to 2.211×10^{16} W/m^2.
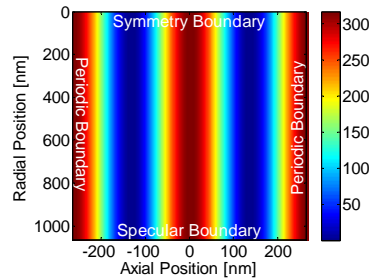

Figure 1 SMILE simulation domain and maximum potential well depth [K] for 20 mJ pump pulses

III. Experimental Setup

The experimental setup can be seen in Figure 2. The output beam from a frequency doubled narrowband Nd:YAG laser (Continuum Powerlite 8010) was split using a polarizing beam splitter to create the counter-propagating pumps which formed the optical lattice. Pump 2 was rotated 90° to achieve the same polarization (S-polarized) as pump 1. The pump laser had a linewidth of 0.003 cm^{-1} and a pulse width of approximately 5 ns. Each pump beam was passed through a 400 mm plano-convex lens which focused each pulse to a diameter (I_{FWHM}) of approximately 15 μm. Care was taken to match the path lengths so that the peak of each pulse arrived at the focal point at approximately the same time. Due to gas breakdown constraints, each pump had a maximum of 25 mJ of energy per pulse. The density perturbations induced by the optical lattice were probed using a separate, broadband frequency doubled Nd:YAG laser (Continuum Minilite). The probe laser produced a 12 mJ pulse over 5 ns and was rotated so that the polarization was perpendicular to the pump beams so as not to interact with the lattice. The probe beam was passed through the same set of lenses directly counter to pump 2 as shown in Figure 2 and obtained a focal diameter of approximately 40 μm. Due to phase matching conditions, the scattered signal from the probe propagates back directly opposite pump 1 as shown in Figure 2. The scattered signal was detected using a Newport 818-BB-45 photodiode and a LeCroy WaveRunner 64Xi oscilloscope. The area under the time dependent intensity profile was taken as the measurement of merit for the experiment. The control of the two lasers, both internal operation and overall timing, was managed using a trio of Stanford Research Systems DG535 delay generators with timebases accurate to better than 50 ps. Total power for the scattered signal was less than 1% of the probe energy. The position and size of the pump and probe pulses was verified using a knife edge power measurement system.
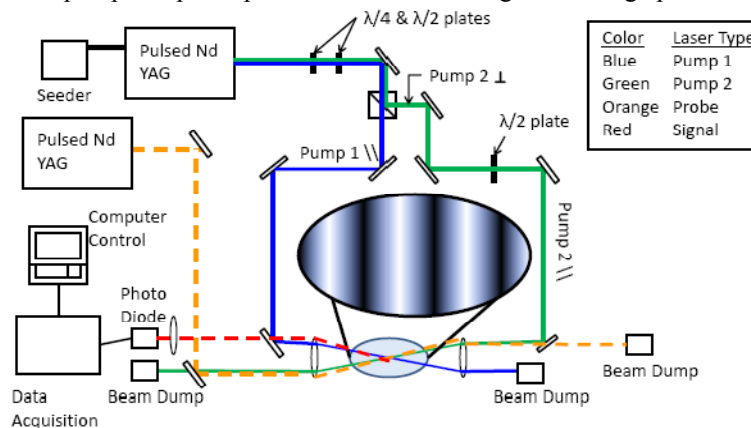

Figure 2 Experimental optical setup

American Institute of Aeronautics and Astronautics

A small vacuum chamber was placed between the two lenses so that the focal points of the two pump beams and probe beam were contained inside the chamber. The vacuum chamber was evacuated to less than 1 mTorr and back filled with research grade N_2. Pressure was measured using an MKS Baratron with a full range of 1000 Torr and a repeatability and linearity of 0.1% full range and accuracy of 1% of the measurement. Optical access to the chamber was provided by two anti-reflective coated (532 nm) laser quartz windows. Scattered signal strength measurements were taken as a function of gas sample pressure and pump beam intensity. Pressure variation in the chamber ranged from 50 to 800 torr and was accomplished by pumping out part of the backfilled nitrogen. The pump intensities varied from 2 mJ (per pump beam per pulse) to 25 mJ, just below the breakdown threshold for nitrogen at the highest pressure. Power variation was accomplished by varying the laser energy let into the system through a half wave plate and polarizing beam splitter shown in Figure 2. The system was allowed to run for 35 seconds to stabilize and the last 300 shots were averaged for better statistics.

It should be noted that the measurement of the scattered signal on the photodiode precludes an assessment of the total or spatially dependant scattering efficiency of the laser induced perturbations. The photodiode only reports the intensity of the light which impinges on its sensor, which may or may not be the entirety of the scattered signal. Furthermore, the probe pulse and pump laser induced perturbations vary as a function of space in the radial direction. However, the setup is sufficient to compare macro-parameters of the experiment such as gas pressure and laser pulse energy by interrogating the same part of the scattered signal shot to shot

IV. Results and Discussion

An example of the density flow field within the domain can be seen in Figure 3 (A) with the radially averaged density shown in Figure 3 (B). Since the domain is axisymmetric, this represents a cylinder around the central axis of the counter propagating laser pulses. The density perturbations simulated by the code are significant compared to the ambient condition, approximately 40 percent of the ambient value. While the magnitude of the density perturbation is not directly measured by the experimental setup, the relative change in that perturbation (squared) is characterized by a corresponding change in signal intensity. Therefore the absolute magnitude of the density perturbations are not further presented.
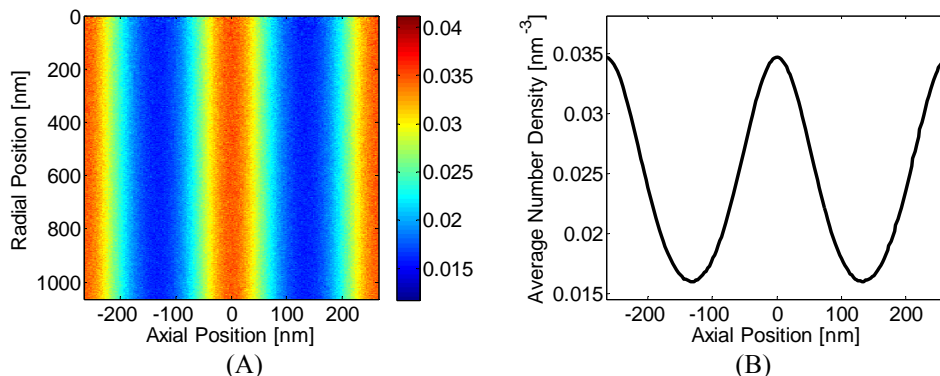

(A)   (B)

Figure 3 A) simulated number density [nm^{-3}] in 760 torr N_2, and B) radially averaged value [nm^{-3}] of (A)

While the long term objective of this research is to enable an arbitrary and tunable, laser based, high temperature neutral gas production capability, the purpose of this particular study was to experimentally show a direct modification of the gas using pulsed lasers and to compare those results with developed numerical models. This is an essential step towards optimizing and characterizing an eventual system. Keeping in mind the un-optimized state of the current setup, with respect to gas heating, an example of the simulated translational temperature field within the domain can be seen in Figure 4 (A) with the radially averaged temperature shown in Figure 4 (B). Since the domain is axisymmetric, this represents a cylinder around the central axis of the counter propagating laser pulses. While the density perturbations are large fractions of the ambient condition, the relative temperature change in the system is small. This is mainly due to the adiabatic timeframe for the turn-on and turn-off of the forcing field. The temporal Gaussian envelope of the laser pulses is long compared to the travel time of a molecule from one side of the potential well to the other. This effectively moves the molecules towards the center of the potentials without significant heating. In future iterations of neutral gas heating experiments, variation in the temporal profile, depth of the potential well, and multiple passes can be investigated to help reach the goal of high temperature (> 2000 K) neutral gases.
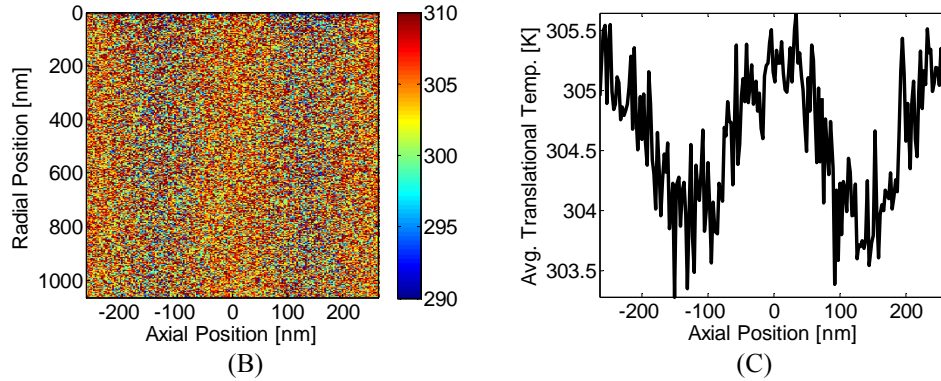
American Institute of Aeronautics and Astronautics

(B)   (C)

Figure 4 A) simulated translational temperature [K] in 760 torr N_2, and B) radially averaged value [K] of (A)

A comparison between the experimental and numerical data can be seen below for two experimental data sets which vary ambient gas pressure and pump laser intensity (pulse energy). In order to make a qualitative comparison, the experimentally recorded signal intensity has been scaled by the circled experimental point. That point was the largest signal with the closest match between experimental and numerical conditions. The numerically simulated density perturbation squared, shown to be proportional to the scattered signal [23], has also been scaled by the circled numerical point. This artificially requires the two circled points to match magnitude at unity. This does not preclude comparison of the data to identify consistent trends with changes in the respective variables. Figure 5 (A) shows an experimental set of data taken at $I_1*I_2 = 1.28 \pm 0.02 \times 10^{32}$ W^2/m^4, varying pressure from 49.5 to 800 Torr and a numerically simulated set of data taken at $I_1*I_2 = 4.89 \pm 0.02 \times 10^{32}$ W^2/m^4, varying pressure from 100 to 760 Torr. The differences in laser intensities can be shown to be linearly proportional and thus fall out when scaled. Figure 5 (B) shows an experimental set of data taken at 760 Torr, varying combined intensity from 8.96×10^{29} to 4.17×10^{32} W^2/m^4 and a numerically simulated set of data taken at 760 Torr, varying combined intensity from 2.17×10^{32} to 4.89×10^{32} W^2/m^4.
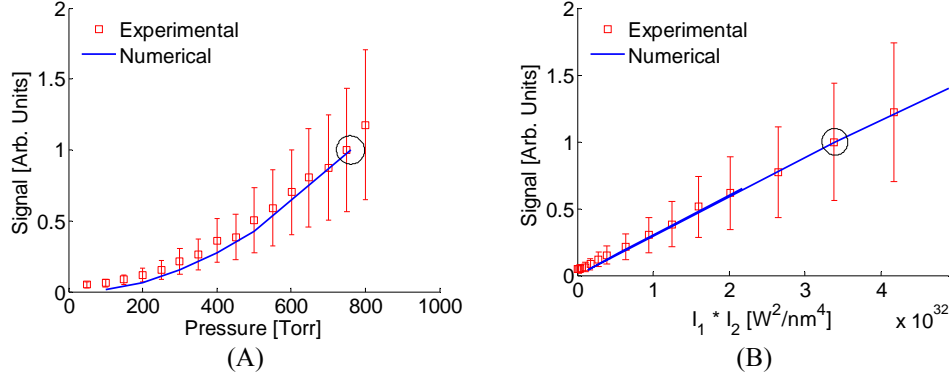

(A)   (B)

Figure 5 Experimental signal intensity and numerical density perturbation vs. A) N_2 pressure and B) pump intensity

The experimental error bars represent one standard deviation above and below an average of 300 points. The large statistical scatter in the recorded data is primarily due to the shot to shot instability in the probe laser's profile both in time and intensity. Figure 6 shows the average of the experimental laser profiles for the pump and probe pulses and the statistical averaging of 300 points. The centers of the points have been offset by 5 ns in either direction in order to show each profile more distinctly. Again, the error bars represent one standard deviation above and below the averaged point. Future experimentation will use two Powerlite 8010 lasers with fairly stable temporal pulse profiles in order to reduce the error bars and obtain a more consistent signal.
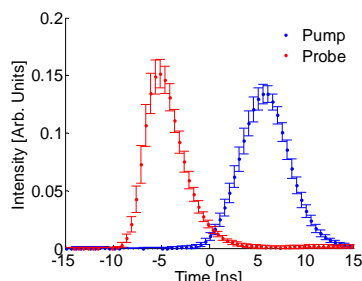
6

American Institute of Aeronautics and Astronautics
Distribution A: Approved for Public Release. Distribution Unlimited

Figure 6 Pump and probe intensity vs. time

V. Conclusion

The presented study compared the effect of counter-propagating pulsed lasers on molecular nitrogen using numerical and experimental methods. A modified version of the DSMC code, SMILE was used to calculate the magnitude of the density perturbations caused by non-resonant pulsed optical lattices in a configuration consistent with previous coherent Rayleigh-Brillouin scattering experiments. Computations were performed for molecular nitrogen with ambient pressures ranging from 100 torr to 760 torr and laser energies from 5 mJ to 25 mJ per pulse. A complimentary coherent Rayleigh-Brillouin scattering experiment was performed in which the scattered signal from the lattice induced gas gratings was measured as a function of ambient pressure and pump energy. The results obtained from the numerical study were scaled and compared to the experiment. Both methods show that the density perturbations (numerical)/scattered signal (experimental) vary linearly with combined laser intensity (I_1*I_2) and quadratic with pressure. Therefore, assuming that the signal of an experiment is proportional to the probe intensity and the square of the density perturbations induced by the pump lasers, the results of the experiment qualitatively support the predictions of the numerical simulations.

Acknowledgments

References

1 Zel'Dovich, Ya. B., and Raizer, Yu. P. Physics of shock waves and high-temperature hydrodynamic phenomena, New York: Academic Press, (1966/1967)

2 Garscadden, A., Kushner, M. J., and Eden, J. G., *IEEE Transactions on Plasma Science.* **19**, pp. 1013-1031

3 Soloukhin, R.I., Shock Waves and Detonations in Gases, Mono Books, Baltimore, (1966)

4 Petersen, E.L, Davidson, D.F., Rohrig, M., and Hanson, R.K., *Proceedings of the 20th International Symposium on Shock Waves*, (1995), pp. 941-946

5 Mahmood, Z., Hussain, I., Linney R., and Russell, D., *J. Anal. and Appl. Pyrolysis*, **44**, (1997), pp. 29-48

6 Shaub, W., and Bauer, S., *Int. J. Chem. Kinetics*, **7**, (2004), pp. 509-529

7 Lilly T., Gimelshein S., Ketsdever A., and Shneider M., "Energy Deposition into a Collisional Gas from Optical Lattices Formed in an Optical Cavity," *Proceedings of the 26th International Symposium on Rarefied Gas Dynamics*, ed. T. Abe, (AIP, New York, 2009), pp. 533-538

8 Lilly T., Ketsdever A., and Gimelshein S., "Resonant Laser Manipulation of an Atomic Beam," *Proceedings of the 27th International Symposium on Rarefied Gas Dynamics*, ed. D. Levin, (AIP, New York, 2011)

9 Lilly, T. C., "Simulated nonresonant pulsed laser manipulation of a nitrogen flow," *Appl. Phys. B* [online journal], 15 Feb. 2011

10 Boyd R. W., Nonlinear Optics, 1st ed. Academic Press, Inc., San Diego, 1992, , pp. 328

11 Kuga, T., Torii, Y., Shiokawa, N. and Hirano, T., "Novel Optical Trap of Atoms with a Doughnut Beam," *Physical Review Letters* Vol. 78, No. 25, 23 June, 1997, pp. 4713-4716

12 Dotsenko, I., Alt, W., Khudaverdyan, M., Kuhr, S., Meschede, D., Miroshnychenko, Y., Schrader, D., and Rauschenbeutel, A., "Submicrometer Position Control of Single Trapped Neutral Atoms," *Physical Review Letters* Vol. 95, No. 3, 13 July, 2005, 033002

13 Schrader, D., Kuhr, S., Alt, W., Mueller, M., Gomer, V., and Meschede, D., "An optical conveyor belt for single neutral atoms," *Applied Physics B* Vol. 73, No. 8, 23 Nov., 2001, pp. 819-824

American Institute of Aeronautics and Astronautics

14 Metcalf, H. J., and van der Straten, P., *Laser Cooling and Trapping*, Springer-Verlag, New York, 1999

15 Takekoshi, T., Yeh, J. R., and Knize, R. J., "Quasi-electrostatic trap for neutral atoms ," *Optical Communications* Vol. 114, No. 5-6, 15 Feb., 1995, pp. 421-424.

16 Grinstead, J. H., and Barker, P. F., "Coherent Rayleigh Scattering," *Phys. Rev. Lett.*, Vol. 85, No. 6, 7 Aug. 2000, pp. 1222-1225

17 Pan, X., Shneider, M. N., and Miles, R. B., "Coherent Rayleigh-Brillouin Scattering," *Phys. Rev. Lett.*, Vol. 89, No. 18, 28 Oct. 2002

18 Shneider, M. N., and Barker, P. F., "Optical Landau damping," *Phys. Rev. A*, Vol. 71, No. 5, 10 May 2005

19 Shneider, M. N., Barker, P. F., and Gimelshein, S. F., "Molecular transport in pulsed optical lattices," *Appl. Phys. A*, Vol. 89, No. 2, 2 May 2007, pp. 337-350

20 Stampanoni-Panariello, A., Kozlov, D. N., Radi, P. P., and Hemmerling, B., "Gas phase diagnostics by laser-induced gratings I. theory," *Appl. Phys. B*, Vol. 81, No. 1, 3 June 2005, pp. 101-111

21 Stampanoni-Panariello, A., Kozlov, D. N., Radi, P. P., and Hemmerling, B., "Gas-phase diagnostics by laser-induced gratings II. Experiments," *Appl. Phys. B*, Vol. 81, No. 1, 3 June 2005, pp. 113-129

22 Kastberg, A., Phillips, W. D., Rolston, S. L., Spreeuw, R. J. C. and Jessen, P. S."Adiabatic Cooling of Cesium to 700 nK in an Optical Lattice," *Physical Review Letters*, vol. 74, no. 9, pp. 1542-1545, February 1995

23 Pan, X., Shneider, M. N., and Miles, R. B., "Coherent Rayleigh-Brillouin scattering in molecular gases," *Phys. Rev. A*, Vol. 69, No. 3, 22 March 2004

24 Ivanov, M. S., and S. F. Gimelshein, *23rd International Symposium on Rarefied Gas Dynamics*, 2003, pp. 339-348

25 Bird, G. A., *Molecular Gas Dynamics and the Direct Simulation of Gas Flows*, Oxford University Press, New York, 1994

26 Ivanov, M. S., et al., *Thermophysics and Aeromechanics*, Vol. 4, 1997, pp. 251-268

27 Borgnakke, C., and Larsen, P. S., "Statistical collision model for Monte Carlo simulation of polyatomic gas mixture," *Journal of Computational Physics*, Vol. 18, No. 4, Aug. 1975, pp. 405-420

28 D I Rosen and G Weyl, "Laser-induced breakdown in nitrogen and the rare gases at 0.53 and 0.357 μm," *Journal of Physics D: Applied Physics*, vol. 20, no. 10, pp. 1264-1276, October 1987

American Institute of Aeronautics and Astronautics
Distribution A: Approved for Public Release. Distribution Unlimited